Journal of Hydroscience and Hydraulic Engineering
Vol. 13, No. 1, May, 1995, 13-24

# REFINED PSI-CELL MODEL FOR INTERPHASE AND INTERPARTICLE MOMENTUM TRANSFER IN BED-LOAD LAYER

By

Hitoshi GOTOH

Research Associate, Department of Civil Engineering, Kyoto University
Yoshida Honmachi, Sakyo-ku, Kyoto, 606, Japan

Tetsuro TSUJIMOTO

Associate Professor, Department of Civil Engineering, Kanazawa University
2-40-20, Kodatsuno, Kanazawa, 920, Japan

and

Hiroji NAKAGAWA

Professor, Department of Global Environmental Engineering, Kyoto University
Yoshida Honmachi, Sakyo-ku, Kyoto, 606, Japan

## ABSTRACT

Bed-load layer is described as the solid/liquid two phase flow, where the phenomena are constituted by the following key-elements: (i) the random motion of the bed-load particle due to the irregular collision and repulsion at the bed surface; (ii) the interphase momentum transfer; and (iii) the interparticle collision. The random motion of bed-load particle is described by the irregular successive saltation model and the PSI (Particle-Source-In)-cell model is introduced to express the interphase momentum transfer. Then the PSI-cell model is modified by taking account of the effect of the interparticle collision on the trajectories of saltation. The simulation based on the present model agrees well with the experiment on the existing probability density and the velocity profile of the saltating particle.

## INTRODUCTION

Figure 1 shows the constitution of the bed-load layer as a solid/liquid two-phase flow. The mechanism for supporting the individual saltation is explained as follows. The momentum is provided from the liquid phase to accelerate saltating particles mostly in the streamwise direction; and the irregular collision and repulsion at the bed surface transforms the direction of the momentum from the streamwise to the upward vertical. The provision of the momentum from liquid phase to solid phase is explicitly described by the drag term in the equation of motion of saltating particles, hence, the key of the model of the individual saltation is how to express the irregular collision and repulsion at the bed surface. The stochastic simulation is a proper approach to describe the irregu-

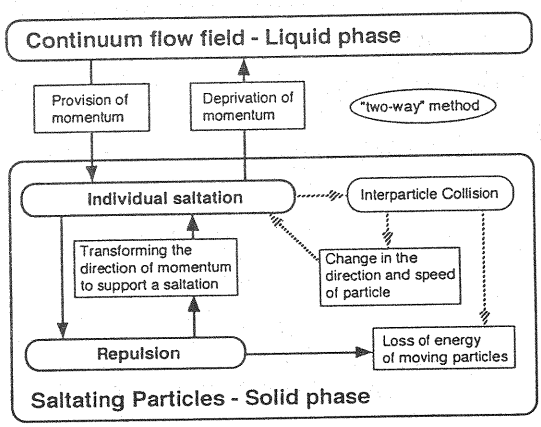


Fig. 1 Constitution of bed-load layer

larity of the contact between saltating particle and bed material particles. Tsujimoto and Nakagawa (1), Sekine and Kikkawa (2), Wiberg and Smith (3) performed the numerical simulation of irregular successive saltation from the viewpoint of stochastic model, where the bed load transport process was described as an ensemble set of successive saltations. To simulate the irregular collision and repulsion at the bed surface, Tsujimoto and Nakagawa (1), Wiberg and Smith (3) employed the two dimensional hypothetical repulsive plane, while Sekine and Kikkawa (2) considered the collision with simulated bed surface composed by random arranged particles.

Another important feature of the bed-load transport process is the existence of the bed-load layer: the bed-load particles are transported within a thin layer nearby bed surface. Hence, under the high bed shear stress, the concentration of bed-load particle becomes sufficiently high so that the momentum transfer between solid and liquid phases is not negligible. A possible way to represent the interaction between solid and liquid phase is coupling a Lagrangian model of saltation with an Eulerian model of the flow. Crowe, Sharma and Stock (4) proposed the Particle-source-in (PSI)-cell model for the Euler-Lagrange coupling and performed the numerical simulation of gas-droplet flow. Nakagawa, Tsujimoto and Gotoh (5) fulfilled the numerical simulation of the bed-load layer based on the PSI-cell model. In their simulation, the negative source of the momentum, which indicated the existence of saltating particle, was added in the governing equation of the flow field, and was evaluated by computing the efflux rate of momentum due to the motion of saltating particles from each control volume of the flow field.

The other important feature of the bed-load transport process is the interparticle collision: the saltating particles confined in the bed-load layer may frequently collide with each other under the high bed shear stress to change their moving directions and velocities. The most straightforward approach to this phenomena is the simulation of granular materials proposed by Campbell and Brennen (6). They assumed the granular material as the group of cylinders and numerically traced the motion of cylinders flowing down along an inclined channel, with considering the inter-cylinder collision. Gotoh, Tsujimoto and Nakagawa (7) conducted the numerical simulation of bed-load particles on the basis of the granular-materials simulation by Campbell and Brennen, where, the motion of the multiple saltating particles were traced simultaneously with considering the interparticle collisions and the irregular collision and repulsion at the bed surface. Although such an approach is accurate, it spends much time in CPU when it is coupled with PSI-cell model for the interphase momentum transfer. Instead, an approximate method for the estimation of the effect of interparticle collision is derived in this paper, which is based on the Lagrangian simulation of the motion of single particle and it is coupled with modified PSI-cell model.

## MODEL FOR INTERPHASE MOMENTUM EXCHANGE IN SALTATION LAYER

*Model of continuum flow (liquid phase):*

Eularian approach is applied to the continuum flow (liquid phase) by solving the governing equations of vertical two-dimensional k-ε turbulence model, in which the effect of the saltating particles is considered through the additional terms in momentum equations. Then the governing equations for the continuum flow phase in vertical two-dimensional flow are written as follows:

$$\frac{\partial U}{\partial x}+\frac{\partial V}{\partial y}=0 \tag{1}$$

$$U\frac{\partial U}{\partial x}+V\frac{\partial U}{\partial y}=g\left(\sin\theta-\frac{\partial h}{\partial x}\cos\theta\right)-\frac{\partial}{\partial x}\left(\frac{P}{\rho}\right)+\frac{\partial}{\partial x}\left(2\Gamma\frac{\partial U}{\partial x}\right)+\frac{\partial}{\partial y}\left\{\Gamma\left(\frac{\partial U}{\partial y}+\frac{\partial V}{\partial x}\right)\right\}+S_{PU} \tag{2}$$

$$U\frac{\partial V}{\partial x}+V\frac{\partial V}{\partial y}=-\frac{\partial}{\partial y}\left(\frac{P}{\rho}\right)+\frac{\partial}{\partial x}\left\{\Gamma\left(\frac{\partial U}{\partial y}+\frac{\partial V}{\partial x}\right)\right\}+\frac{\partial}{\partial y}\left(2\Gamma\frac{\partial V}{\partial y}\right)+S_{PV} \tag{3}$$

$$U\frac{\partial k}{\partial x}+V\frac{\partial k}{\partial y}=\frac{\partial}{\partial x}\left\{\left(\nu+\frac{\nu_t}{\sigma_k}\right)\frac{\partial k}{\partial x}\right\}+\frac{\partial}{\partial y}\left\{\left(\nu+\frac{\nu_t}{\sigma_k}\right)\frac{\partial k}{\partial y}\right\}+G+\varepsilon \tag{4}$$

$$U\frac{\partial \varepsilon}{\partial x}+V\frac{\partial \varepsilon}{\partial y}=\frac{\partial}{\partial x}\left\{\left(\nu+\frac{\nu_t}{\sigma_\varepsilon}\right)\frac{\partial \varepsilon}{\partial x}\right\}+\frac{\partial}{\partial y}\left\{\left(\nu+\frac{\nu_t}{\sigma_\varepsilon}\right)\frac{\partial \varepsilon}{\partial y}\right\}+\frac{\varepsilon}{k}(C_{1\varepsilon}G+C_{2\varepsilon}\varepsilon) \tag{5}$$

$$G=\nu_t\left[2\left\{\left(\frac{\partial U}{\partial x}\right)^2+\left(\frac{\partial V}{\partial y}\right)^2\right\}+\left(\frac{\partial U}{\partial y}+\frac{\partial V}{\partial x}\right)^2\right] \quad ; \quad \Gamma=\nu_t+\nu \quad ; \quad \nu_t=C_\mu\frac{k^2}{\varepsilon} \tag{6}$$

where, $x,y$=the streamwise and upward vertical coordinates, respectively; $U,V$=mean velocity components in $x,y$ directions, respectively; $P$=deviation from hydrostatic pressure; $h$=flow depth; $\rho$=mass density of fluid; $g$=gravitational acceleration; $\theta$=averaged bed slope; $S_{PU},S_{PV}$=sink terms for the interphase momentum transport; $\Gamma$=effective viscosity; $\nu$=kinematic viscosity; $\nu_t$=eddy kinematic viscosity, and $G$=production of turbulence energy. The empirical constants are set at the recommended value by Launder & Spalding (8) as follows: $C_\mu$=0.09, $C_{1\varepsilon}$=1.44, $C_{2\varepsilon}$=1.92, $\sigma_k$=1.0 and $\sigma_\varepsilon$ =1.3.

The effect of saltating particles is transferred through the additional source terms $S_{PU},S_{PV}$ in the momentum conservation equations. These additional terms bring other unknown correlation terms in $k$- and $\varepsilon$-equations, and it requires some models with empirical constants to make the governing equations closed to be solved. Although the models of unknown correlation terms in $k$-and $\varepsilon$-equations should be verified experimentally, the deficiencies of experimental technique prevent from precise measurement of the turbulent structure in bed-load layer. In this study, the unknown correlation terms in $k$-and $\varepsilon$-equations are not considered, therefore, the solution of turbulent field is not directly influenced by the saltating particles but affected through the change of the mean velocity field by the additional momentum source terms $S_{PU},S_{PV}$.

*Model of saltating particles (solid phase):*

The most important aspect of saltation model is the description of irregular motion of saltating particles due to the collision and repulsion at the bed surface. Tsujimoto and Nakagawa (1) proposed the simulation of successive saltation, in which the irregularity of collision and repulsion at the bed surface is expressed by the hypothetical repulsing plane. In this study, their stochastic model is modified and generalized.

The trajectory of the saltation is governed by the following equations.

$$\rho\left(\frac{\sigma}{\rho}+C_M\right)A_3d^3\frac{du_p}{dt}=\frac{1}{2}C_D\rho A_2d^2\sqrt{(U-u_p)^2+(V-v_p)^2}\,(U-u_p) \tag{7}$$

$$\rho\left(\frac{\sigma}{\rho}+C_M\right)A_3d^3\frac{dv_p}{dt}=\frac{1}{2}C_D\rho A_2d^2\sqrt{(U-u_p)^2+(V-v_p)^2}\,(V-v_p)-\rho\left(\frac{\sigma}{\rho}-1\right)gA_3d^3 \tag{8}$$

$$C_D=C_{D\infty}+\frac{24}{R_e} \quad ; \quad R_e=\frac{d\sqrt{(U-u_p)^2+(V-v_p)^2}}{\nu} \tag{9}$$

where, $d$=diameter of saltating particle; $u_p,v_p$=streamwise and upward vertical components of velocity of the saltating particle, respectively; $C_M$=added mass coefficient; $\sigma$=mass density of saltating particle; $A_2,A_3$=two-and three-dimensional geometrical coefficients, respectively; and $C_D$=drag coefficient. The parameter $C_{D\infty}$ depends on the shape of the particle: $C_{D\infty}$=0.4 for a sphere; and $C_{D\infty}$=2.0 for the natural sand recommended by Rubey (9). The experimental evidence indicates that the effect of turbulence on the trajectory of saltation is not significant (Tsuchiya and Aoyama (10); Nakagawa, Tsujimoto and Akao (11)), consequently, the flow velocity in a drag coefficient $C_D$ is evaluated by the mean velocities $U,V$.

Figure 2 shows a definition sketch of the collision and repulsion at an bed surface. The change in the velocity of the saltating particle is written as:

$$\begin{bmatrix}u_{gout}\\ v_{gout}\end{bmatrix}=\begin{bmatrix}e\cdot\cos^2\alpha-f\cdot\sin^2\alpha & (e+f)\cos\alpha\sin\alpha\\ (e+f)\cos\alpha\sin\alpha & e\cdot\sin^2\alpha-f\cdot\cos^2\alpha\end{bmatrix}\begin{bmatrix}u_{gin}\\ v_{gin}\end{bmatrix} \tag{10}$$

where $(u_{gin}, v_{gin})$, $(u_{gout}, v_{gout})$=velocity components of saltating particle just before and after collision, respectively; and $\alpha$=angle of the hypothetical repulsing plane against the mean bed surface. The parameter $\alpha$ is a probabilistic variable which represents the irregularity of the collision. Even if all of the bed material particles exposed at surface are located at the same elevation, the parameter $\alpha$ is not constant because of the irregularity of colliding point due to the configuration of an individual particle on the bed surface.

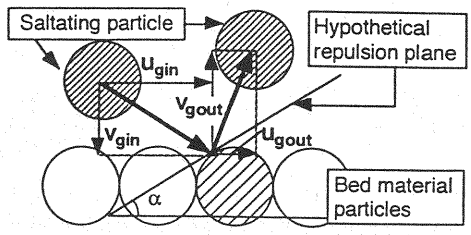


Fig. 2 Definition sketch of collision and repulsion at a bed-surface

*PSI-Cell model for interphase coupling:*

The key of the interphase coupling is how to express the effect of the saltating particle on the continuum flow. One of the solutions of this problem is to adopt the particle-source-in-cell (PSI-cell) model which treats the saltating particle as a source of momentum in the continuum flow field. The flow field is divided into a series of cells, and each cell is regarded as a control volume for the liquid phase. As a saltating particle passes through a given cell, it is accelerated or decelerated and brings the resultant momentum deficiency or augmentation of the flow field.

Figure 3 shows a saltating particle traversing a U-cell "$j$" of flow field. The change in the momentum of saltating particle by traversing the $j$-th cell is defined as the product of particle's mass by the difference in the velocity of the particle at the borders of the cell. And the net efflux rate of the momentum of saltating particles is obtained by averaging the efflux rate for all trajectories of the saltating particles which pass through a given cell. This scenario can be formulated by calculating the efflux rate of the momentum due to the saltating particles as follows:

$$S_{PU_j} = -\frac{1}{N_j}\sum_{i=1}^{N_j}\frac{\sigma}{\rho}q_B w_j\left\{\left(1+\frac{\alpha_p}{R_j}\right)u_{pout_i} - u_{pin_i}\right\}_j \frac{1}{\Delta V_j}$$

$$S_{PV_j} = -\frac{1}{N_j}\sum_{i=1}^{N_j}\frac{\sigma}{\rho}q_B w_j\left\{\left(1+\frac{\alpha_p}{R_j}\right)v_{pout_i} - v_{pin_i}\right\}_j \frac{1}{\Delta V_j} \quad ; \quad w_j = \iint_{\Delta V_j} f_B(x,y)\mathrm{d}V \qquad (11)$$

where $q_B$=sediment discharge; $(u_{pini}, v_{pini})$, $(u_{pouti}, v_{pouti})$=velocity components of the saltating particle coming in and going out the $j$-th cell respectively; $N_j$=the number of the saltating particle traversing the $j$-th cell ; $R_j$=the coefficient of the change in particle's velocity due to the interparticle collision in the $j$-th cell; $\Delta V_j$=volume of the $j$-th cell; $w_j$=coefficient for the distribution of the sediment discharge of the $j$-th cell; $f_B(x,y)$=existing probability density of the saltating particle; and $\alpha_p$=empirical constant discussed below.

The particle, which looses its velocity due to the interparticle collision, recovers the velocity by the momentum provision from the flow field, consequently the additional loss of momentum due to the interparticle collision occurs in the flow field. This effect is taken into account approximately through the parameters $R_j$ and $w_j$. Determination of these parameters will be discussed in the following chapter.

When the flow field is uniform in the streamwise direction, the averaged characteristics of saltating particles is also uniform in the streamwise direction, therefore, the particle's velocity which is required for the estimation of the argumentation of momentum should be recorded on the border of the series of layers parallel to the bed surface. In the uniform flow condition, the cell "$j$" is regarded as the layer "$j$", hence the parameter $w_j$ is rewritten as follows:

$$w_j = \int_{y_{minj}}^{y_{maxj}} f_B(y)\mathrm{d}y \qquad (12)$$

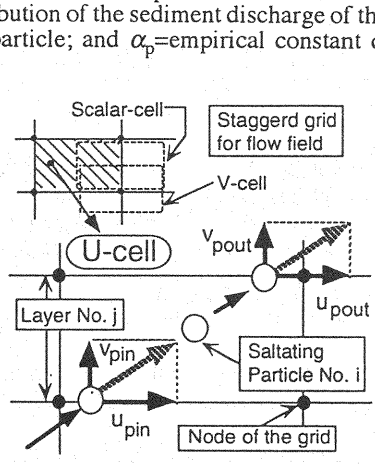


Fig. 3 Saltating particle traversing U-cell

where $y_{maxj}$, $y_{minj}$=upper and lower border of the layer "$j$"; and, $f_B(y)$=existing probability density of the saltating particle.

In general, the interaction term in the momentum equation of flow is calculated by spatially integrating the momentum loss due to the motion of sediment particles over each grid-cell of the flow, hence, the effect of the sediment particles on the flow should be the sub-grid scale one. In the bed-load calculation, to treat the interaction term as a sub-grid scale effect is prevented by the following two contradicting requirements: (i) The bed-load particles are mostly coarse-sediment; and (ii) in the vicinity of the bottom wall, the thin cell for the flow calculation is essential to improve the accuracy of the calculation. Therefore, in the vicinity of the bottom wall, the thickness of the cell for the flow calculation is larger than the diameter of sediment particle, in other word, the effect of the sediment particle on the flow field is not necessary regarded as the sub-grid scale one.

To avoid this contradiction, the time-and-spatially-averaged governing equations of the flow are introduced in this simulation. If the most part of a certain flow cell is occupied by saltating particles at a moment, the particle moves away from the cell in the next-few-time steps, and the cell will be occupied by water. By introducing the long-time-average operation into the governing equation of the flow, the interaction terms of the flow equation can be defined as the ensemble average of the effect of each coarse sediment traversing a flow cell. Based on this definition of the governing equation of the flow, the simulation can be performed even under the condition that the diameter of the sediment is comparable to the thickness of the flow cell.

## MODELING OF INTERPARTICLE COLLISION

Strictly speaking, the interparticle collision should be treated by tracing the multiple particles simultaneously (see Gotoh et al. (7)). Such a straightforward approach requires too much CPU-time to couple with the PSI-cell model for the interphase momentum transfer, which also needs the iterating calculation to get the convergent solution. In this study, to save the CPU-time for calculating the interparticle collision, the effect of the interparticle collision is approximately evaluated on the basis of the motion of the single particle passing through the group of particles, among which the relative position of each particle does not change.

How to estimate the parameters of the interparticle collision, $R_j$ and $w_j$ is shown schematically in Fig. 4. Firstly, the motion of individual particles is traced in the clear water flow (see Fig. 4 [A]), and the existing probability density and velocity profile of the saltating particles are calculated through the statistical operation of the simulation data of the saltation trajectories. Secondly, the group of the saltating particles are arranged based on the existing probability density of saltating particle in the clear water flow (see Fig. 4 [B]). These particles are assumed to move at the respective velocity at each level following the mean velocity profile of the particles. Thirdly, the motion of a single particle passing through the group of the saltating particles are traced on the coordinate system moving at the same velocity as the group of saltating particles at each level, where the relative positions of the group of the saltating particles do not change (see Fig. 4 [C]). Finally, the parameters of the interparticle collision, $R_j$ and $w_j$ are estimated based on the simulated trajectories of a single saltating particle moving through the group of saltating particles. Although the interparticle collision brings about the change of the velocity to the both of the colliding particles, the following assumption is introduced for simplicity: the velocity and the position of the saltating particle included the group of the particles dose not change due to the interparticle collision. This assumption is inevitable to estimate the effect of the interparticle collision based on the trace of a single particle.

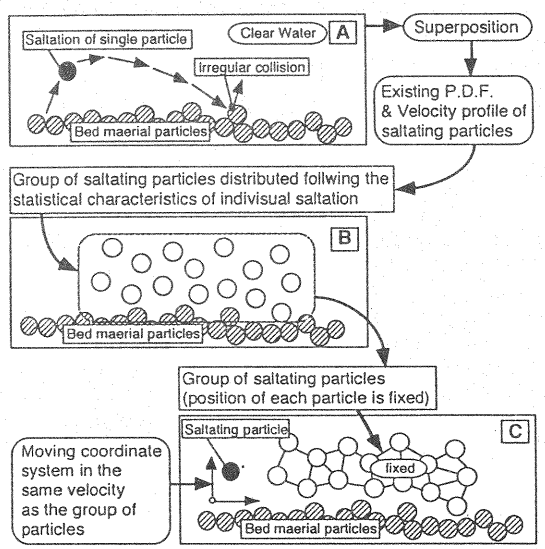


Fig. 4 Estimation of parameters of interparticle collision

Under the situation illustrated in Fig. 4[C], the loss of the momentum of the saltating particle due to the interparticle collision is only

considered, even if the argumentation of the momentum of other saltating particles occurs simultaneously. It means that the effect of the interparticle collision is overestimated there. While, under the situation illustrated in Fig. 4[A], the motion of the individual particle is perfectly independent of the motion of other saltating particles, in other words, the trajectory of the saltation is not affected by the interparticle collision. The real saltation exists between the situations [A] and [C], so that the existing probability density of saltating particle, $f_B(y)$, for the real situation is assumed to be written as follows:

$$f_B(y) = (1-\beta_p) f_B^{\,m}(y) + \beta_p f_B^{\,s}(y) \tag{13}$$

where $f_B^{\,s}(y)$, $f_B^{\,m}(y)$=the existing probability density for the saltation in Fig. 4[A] and [C], respectively; and $\beta_p$=the interpolating parameter for between the both extreme situations [A] and [C]. Under the situation in Fig. 4[C], the momentum of saltating particle is not transferred but lost by the interparticle collision. In this sense, the situation in Fig. 4[C] is more extreme than that in Fig. 4[A], therefore the parameter $\beta_p$ is near the unity. Here it is set 0.9. The parameter as for the existing probability density, $w_j$ is written as follows:

$$\frac{w_j}{w_j^{cl}} = \frac{f_B(y_j)\Delta y_j}{f_B^{\,s}(y_j)\Delta y_j} = \frac{1-\beta_p}{R_{pdf}} + \beta_p \quad ; \quad R_{pdf} \equiv \frac{f_B^{\,s}(y_j)\Delta y_j}{f_B^{\,m}(y_j)\Delta y_j} \tag{14}$$

where $w_j^{cl} = w_j$ for clear water flow. The parameter of the change in velocity due to the interparticle collision, $R_j$, is defined as follows:

$$R_j \equiv \prod_{i=1}^{N_j^{co}} r_{ij} \quad ; \quad r_{ij} = \frac{|\mathbf{u}_{af}|}{|\mathbf{u}_{bf}|} \tag{15}$$

where $N^{co}{}_j$=number of the collision in the $j$-th cell; and $\mathbf{u}_{bf}$,$\mathbf{u}_{af}$=velocity vectors of the particle just before and after collision, respectively. Fig. 5 shows the calculated results of $R_j$ and $R_{pdf}$ (the ratio of the probability density function $f_B^{\,s}$ to $f_B^{\,m}$) under the condition shown in Table 1, where $I_e$=energy gradient; $h$=flow depth; $U_m$=bulk mean velocity of the flow; $u_*$=shear velocity; and $\tau_*$=dimensionless shear stress. Spherical glass beads of the specific gravity 2.60 and the diameter 0.4 cm were used as the test particles in the experiment and the simulation. The coefficients of repulsion is set $e$=$f$=0.75 to get the agreement between the averaged saltation height of the experiment and that of the simulation.

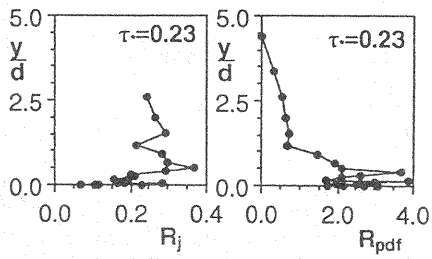


Fig. 5 Distribution of $R_j$ and $R_{pdf}$

## PROCEDURE OF THE SIMULATION AND BOUNDARY CONDITIONS

The procedure of simulation is illustrated in Fig. 6, and explained below. [1] The flow field without containing saltating particles is solved to find the velocity profile of the clear-water flow. [2] The trajectories of the saltating particles in clear-water flow are calculated to estimate the velocity and the existing probability density of saltating particles. [3] The coefficients of the interparticle collision, $R_j$ and $w_j$, are estimated by using the results of the simulation of successive saltation. [4] The source terms of the momentum conservation equation are calculated for each cell throughout the flow field. [5] The flow field is solved incorporating these source terms, and then [6] the trajectories of the saltating particles are estimated again in the corrected flow field and the momentum source terms are updated, thereby completing the cycle of the interaction between solid and liquid phases. This iteration is continued until the discrepancy of the updated solution from the previous one becomes sufficiently small.

Table 1 Condition of experiment

| | | |
|---|---|---|
| energy gradient | Ie | 0.02 |
| flow depth | h | 8.29 cm |
| bulk mean velocity | Um | 144.8 cm/s |
| shear velocity | u* | 13.56 cm/s |
| dimensionless shear stress | τ* | 0.23 |

The technique for solving the governing equations of flow field is an extension of the TEACH code developed by Gosman and Ideriah (12). The governing equations are discretized on the staggard

grid by employing SIMPLE algorithm proposed by Patankar and Spalding (13). An instructive source code is registered in the program library of the Data Processing Center in Kyoto University: "TEACHTB / A general computer code for two-dimensional, turbulent recalculating flows using the two-equation k-ε turbulence model" (originally corded by F.J.K. Ideriah, A.D. Gosman and W.M. Pun, modified by M. Takemoto). The calculated region is covered with 10 (in the streamwise direction) × 16 (in the vertical direction) grid cells. In order to calculate the bed-load layer precisely, the non-uniform grid is adopted in the vertical direction, in which the width of the grid becomes larger gradually from the bed to the free-surface. And, in the streamwise direction, uniform grid is arranged the step-size of which is the same as the flow depth.

The boundary conditions for the calculation are as follows: At the bottom, the well-known wall function is applied. The mean velocity in the streamwise direction, $U_p$, at the lowest point of grid, $y_p$, follows the logarithmic law as follows:

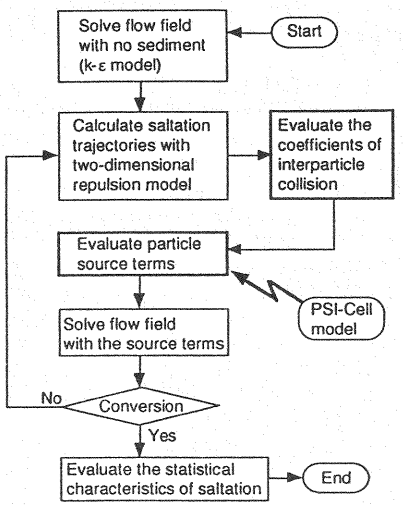


Fig. 6 Procedure of simulation

$$\frac{U_p}{u_*}=\frac{1}{\kappa}\ln\left(\frac{y_p}{k_s}\right)+A_r \qquad (16)$$

where $\kappa$=Kármán constant (=0.41); $k_S$=equivalent roughness height (=$d$); and $A_r$=constant (=8.5 for rough bed). $k$ and $\varepsilon$ at the lowest point of grid are calculated by the local equilibrium assumption ($G=\varepsilon$) and the logarithmic law of velocity profile, as follows.

$$\frac{k_p}{u_*^2}=\frac{1}{\sqrt{C_\mu}}=3.33 \quad ; \quad \varepsilon_p=\frac{u_*^3}{\kappa y_p} \qquad (17)$$

At the free surface, an axial symmetric condition is modified in the following manner: Firstly, the flow field is solved with an axial symmetric condition, in which the free surface is regarded as the central axis of a pipe flow. After that, the boundary condition at the free surface is modified by considering the damping of turbulent energy at the free surface after Nezu and Nakawaga (14) as follows:

$$k_w=D_w\cdot k_a \quad , \quad D_w=0.8 \quad ; \quad \left(\frac{\partial U}{\partial y}\right)_w=\frac{1}{\nu_t}(-\overline{uv})_a \qquad (18)$$

where, $D_w$=damping factor (0.8 is used in this study after an recommendation by Nezu & Nakagawa ); and the subscripts "a" and "w" imply the pipe flow and the open channel flow, respectively. At the upstream end and the downstream end of the calculated field, a periodic boundary condition is employed.

The time interval for calculating the trajectory of a saltating particle, $\Delta t$, is set at 1/500 second as proposed by Nakagawa, Tsujimoto and Gotoh (7). By using this time interval, the trajectory of the standard saltation at $\tau_*$=0.23, whose height corresponds to the averaged height of all samples of saltations, is divided into about 50 steps. Hence fifty sets of the successive saltations are calculated in each cycle of the solid-phase calculation, this condition corresponds to calculating 500 numbers of the individual saltation at $\tau_*$=0.23.

After the alternate iterations of the liquid and solid phases for several times, the discrepancy of the updated flow field solution from predetermined one becomes sufficiently small, and one obtains a convergence of the calculation. The solutions mentioned below are the results after 10th iterations where the convergent condition is satisfied.

The sediment discharge $q_B$ was calculated by the Meyer-Peter and Müller's formula (15) for the given dimensionless bed-shear stress.

## RESULTS AND DISCUSSIONS

*Results of liquid phase:*

Figure 7 shows the velocity distribution of flow containing the equilibrium discharge of sediment for the given dimensionless bed shear stress $\tau_*$. The experimental condition is the same as that shown in Table 1. The bulk-mean velocity, $U_m$, and the water depth, $h$, are given in the calculation, hence these values of the sediment-laden condition are the same as that of clear-water condition. The downward shift of velocity profile in Fig. 7 is caused by the increase of the shear velocity (the denominator of the coordinate), which implies the increase of the energy gradient of the flow. In this figure, flow velocities are normalized by shear velocity, which is estimated as a result of the simulation. The experiment shows a discrepancy of the velocity of sediment-laden flow from that of clear-water flow. Although the tendency of the experiment is clearly simulated by both of the PSI-cell model and the modified PSI-cell model, the PSI-cell model gives an overestimation in the middle region of the flow ($1<y/d<10$). This discrepancy is reduced by the modified PSI-cell model, which takes the interparticle collision approximately into account. The gradient of the velocity profile in the experiment becomes gradually milder with approaching to the bottom. This tendency is caused by the vertical mixing of momentum in bed-load layer promoted by the motion of the saltating particles. Kawamura (16) found out the similar characteristics in the velocity profile of the blown sand layer. As for the brown sand, the relative density of the sand to fluid (air) is about $10^3$ times larger than that of the sediment driven by flowing water, therefore, the effect of the contained sediment in water flow is weaker than that of the air flow.

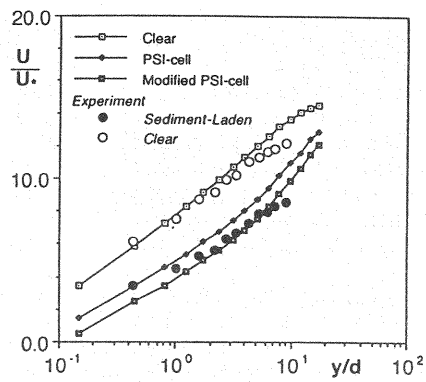


Fig. 7 Flow velocity profile

*Results of solid phase:*

The statistical characteristics of individual saltation are shown in Figs. 8-11. Fig. 8 shows the probabilistic densities of the streamwise velocity component just before a collision at the bed, $u_{gin}$, and that just after a collision, $u_{gout}$. The probability density profile of $u_{gin}$ is skewed: the gradient of a rising limb is smaller than that of falling limb. On the other hand, the probability density profile of $u_{gout}$ is approximately symmetrical, although the some parts of the rising limb are cut off by the line $u_{gout}=0$. Fig. 9 shows the same tendencies which are found in the probability density profiles of $v_{gin}$ and $v_{gout}$, namely, the upward-vertical component just before and after a collision at the bed.

As for the detail of the probability density profiles of the velocity components, the modified PSI-cell model is different from others. Namely, the second peak in the low-speed region of the probability density are found in modified PSI-cell model,

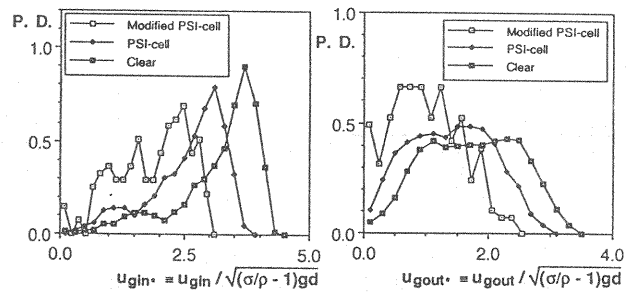


Fig. 8 Velocity of particle just before collision at a bed (streamwise components)

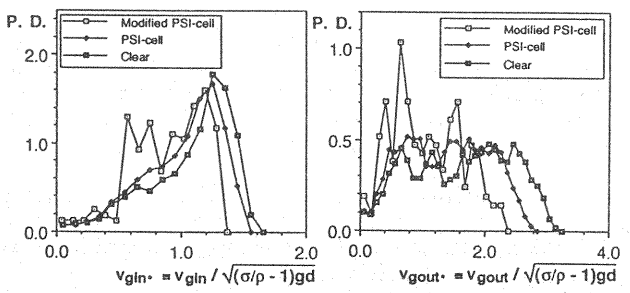


Fig. 9 Velocity of particle just before collision at a bed (upward vertical components)

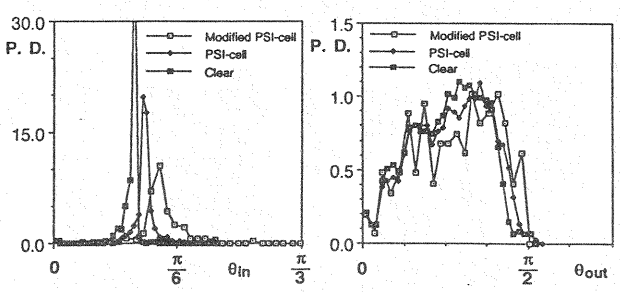


Fig. 10 Angle $\theta_{in}$ and $\theta_{out}$

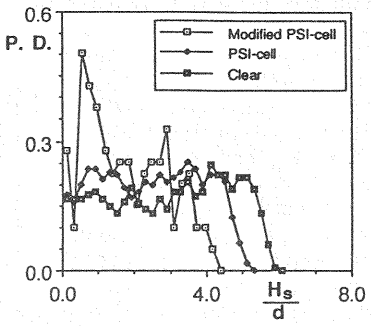


Fig. 11 Height of saltation $H_s$

especially in the probability densities of the upward-vertical velocities $v_{gin}$ and $v_{gout}$.

Figure 10 shows the probability density profile of the angle between depositing direction and streamwise one, $\theta_{in}$; and that of the angle between the repulsing direction and streamwise one, $\theta_{out}$. The angel $\theta_{in}$ distributes with narrow band; while the angle $\theta_{out}$ distributes in a wide range due to the irregularity of the bed surface. The second peak, which was found in the probability density of the characteristic velocities, is also found in the distribution of $\theta_{out}$.

The existence of the second peak in the modified PSI-cell model can be explained by the change in saltation trajectory due to interparticle collisions. The increase in the variation of the angle $\theta_{in}$ diminishes the effect of sheltering among neighboring particles on the bed; and it consequently makes the distributing range of the hypothetical repulsing plane $\alpha$ wide. The variation of the angle $\theta_{in}$ in the modified PSI-cell model is larger than those of the others. In other words, the additional irregularity in the motion of saltating particles caused by the interparticle collision brings the larger value of $\theta_{in}$, which is not found in the individual saltation without collision, and brings the wide-range distribution to the angle $\theta_{in}$. The particles colliding with other saltating particles looses or gains the energy and it collides the bed surface in lower velocity than the particle without interparticle collision. The second peaks found in the distribution of $u_{gin}$ and $v_{gin}$ might be brought by this effect. Fig. 11 shows the probability density of the hight of saltation, the peak of which appears approximately at $H_s/d$=1.0 caused by the interparticle collision.

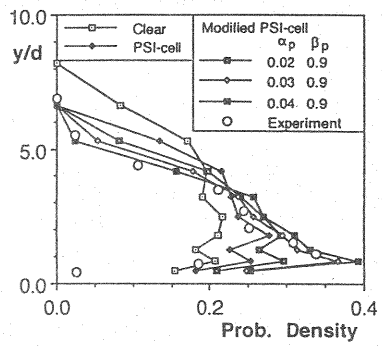


Fig. 12 Existing probability density of particles

In the present model, the motion of the single particle passing through other saltating particles, the relative positions of which are fixed, is traced as illustrated in Fig. 4; therefore the effect of the interparticle collision is considered only for the motion of a traced particle. In other words, the positions and the velocities of other saltating particles do not change due to the interparticle collision. Gotoh, Tsujimoto and Nakagawa (7) found that wider range distribution of $H_s$ is predicted as the result of the simulation of granular materials, in which the motion of the saltating particles with interparticle collision traced simultaneously in clear water flow. In the present simulation, the bed shear stress is set at $\tau_*$=0.23, therefore the discrepancy between the simulation of granular materials and the present simulation is not so small to bring no severe error to the total structure of the flow field.

Figure 12 shows the existing probability density of the saltating particle in the vertical direction calculated under the condition in Table 1, and the result of the experiment in the open channel flume is also shown in this figure. The clear-water flow model gives an overestimation in the upper region of saltation layer and gives an underestimation in the lower region; while the PSI-cell model revises the discrepancy properly to improve the agreement with the experiment. The agreement between simulation and experiment is furthermore improved by introducing the modified PSI-cell model, in which the effect of the interparticle collision is considered.

Figure 13 shows the distribution of the streamwise component of the particle's velocity calculated under the condition in Table 1. The result of the experiment in the open channel flume is also shown in this figure. The clear water flow model shows a significant overestimation, since the clear water flow

model is not able to treat the damping of the drag force acting on the particle caused by the momentum-loss of the flow by containing particles. This tendency becomes remarkable with decreasing the height form a bed, because of the increase of the existing probability of saltating particle. Although better agreements are recognized among the result of the PSI-cell, that of the modified PSI-cell model and the experiment, even the modified PSI-cell models model cannot express the details of the velocity profile of particle. The reason of this discrepancies is regarded as the approximation of the interparticle collision in modified PSI-cell model.

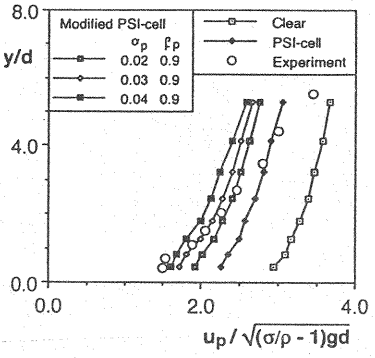


Fig. 13 Velocity of particles

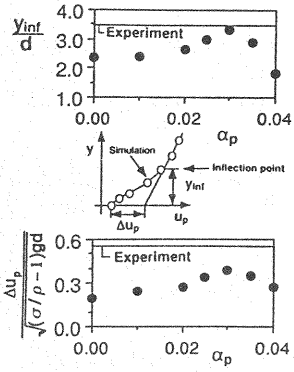


Fig. 14 Verification of modified PSI-cell model

The modified PSI-cell model includes the empirical constant $\alpha_p$. Fig. 14 shows the verification of constant $\alpha_p$ by considering the characteristics of the velocity distribution of particle in the near-bottom region. The height of the inflection point found in the velocity distribution and the deviation of the velocity at the bottom schematically shown in this figure are compared with each other against the value of $\alpha_p$. The simulation gets the best agreement with the experiment at $\alpha_p$=0.03.

## CONCLUSIONS

PSI-cell model for describing the bed-load layer as a two-phase flow is revised by considering the additional effect due to the interparticle collision. The results obtained in this paper are summarized below:

(1) The solid phase is expressed by the stochastic model of irregular successive saltation; while the liquid phase is described by the k-ε model of turbulence with the momentum sink term. To connect those two phases, PSI-cell model is adopted.

(2) To evaluate the effect of interparticle collision on the interphase momentum transfer, PSI-cell model is modified. The coefficients of the modification of PSI-cell model are evaluated on the basis of the motion of a single particle among other saltating particles, the relative positions of which do not change.

(3) The velocity profile of the flow in bed-load layer is calculated. The experimental result on the change in velocity profile by containing the sediment is explained fairly well by the present simulation.

(4) The probability densities of the characteristic quantities of the individual saltation (particle's velocities before and after collision with the bed, saltation height and so on) are predicted by the present simulation. The effect of the interparticle collision on the motion of the individual saltation is considered by comparing the results of the PSI-cell with that of modified PSI-cell model. Each probability density of the characteristic quantities predicted by PSI-cell model has a single peak; while the prediction by the modified PSI-cell model has another peak, which indicates the change in the trajectory of saltation due to the interparticle collision.

(5) The existing probability density of saltating particles is also predicted by the present simulation. Although the prediction of PSI-cell shows a better agreement with the experiment than the clear water flow model, the modified PSI-cell model improves the accuracy of the prediction furthermore.

(6) The velocity profile of the saltating particle is also predicted by the present simulation. The experiment indicates the change in the velocity gradient near the bottom, or an inflection point, appears there. This tendency is fairly well explained by the modified PSI-cell model.

Most part of this paper was published in Japanese (17), but revised herein.

## ACKNOWLEDGMENT

The authors wish to express their gratitude to Messrs. M. Watanabe and Y. Inoue (Graduate Students, Kyoto Univ.) for their helps with the experiment and the data processing.

## REFERENCES


1. Tsujimoto, T. and Nakagawa, H.: Stochastic Study on Successive Saltation by Flowing Water, *Proc. 2nd Int. Sym. on River Sedimentation,* Nanjing, Chaina, pp. 187-201, 1983.
2. Sekine, M. and Kikkawa, H.: Mechanics of Saltating Grains, *Jour. Hydraulic Engrg., ASCE,* Vol. 118, No.4, April, pp.536-558, 1992.
3. Wiberg, P. L. and Smith, D. J.: A theoretical model for saltating grains in water, *Jour. Geophys Res.*, 90(4), 7341-7354, 1987.
4. Crowe, C. T., Sharma, M. P. and Stock, D.E. :The Particle-Source-In Cell (PSI-CELL) Model for Gas-Droplet Flows, *Jour. Fluids Engrg.*, ASME, June, pp.325-332, 1977.
5. Nakagawa, H., Tsujimoto, T. and Gotoh, H.: Numerical simulation of bed-load layer as two-phase flow, *Int. Conf. Hydro-Sci. and Engrg.*, Washington D.C., USA, pp.638-645, 1993.
6. Campbell, C. S. and Brennen, C. E.: Computer simulation of granular shear flows, *Jour. Fluid Mech.*, Vol. 151, pp.167-188, 1985.
7. Gotoh, H., Tsujimoto, T. and Nakagawa, H.: Numerical model of granular material for the dynamics of bed-load layer, *Proc. XXV IAHR Cong.*, Tokyo, Japan, B-1-4, pp. 33-40, 1993.
8. Launder, B. E. and Spalding, D. B.: The Numerical Computation of Turbulent Flow, *Computer Method in Applied Mech. and Engrg.*, Vol. 3, pp.269, 1974.
9. Rubey, W. W.: Settling Velocities of gravel, sand and silt, *American Jour. Science* Vol. 25, No.148, 1933.
10. Tsuchiya, Y. and Aoyama, T.: On the mechanism of saltation of a sand particle in a turbulent stream (2), *Annu. Disas. Prev. Res. Inst. Kyoto Univ.*, 13B, pp.199-216 , 1970 (in Japanese).
11. Nakagawa, H., Tsujimoto, T. and Akao, T.: Stochastic Behaviors of Saltating Particles, *Proc. 27th Jap. Conf. Hydraul., JSCE*, 1983 (in Japanese).
12. Gosman, A. D. and Ideriah, J. K.: TEACH-T, A General Computer Program for Two-Dimensional Turbulent Recirculating Flows, Dept. of Mech. Engrg., Imperial College of Tech., London, S.W. 7, 1976.
13. Patankar, S. V. and Spalding, D. B.: A Calculation Procedure for Heat, Mass and Momentum Transfer in Three-Dimensional Parabolic Flows, *Int. Jour. Heat Mass Transfer*, 15, pp.1787-1806, 1972.
14. Nezu, I. and Nakagawa, H. : Numerical Calculation of Turbulent Open-Channel Flows by Using a Modified k-ε turbulence model, *Proc. JSCE*, No.387, pp.125-134, 1987 (in Japanese).
15. Meyer-Peter, E. and Müller, R.: Formulas for bed-load transport, *Proc. 2nd IAHR Congr.*, Stockholm, pp.39-64 , 1948 .
16. Kawamura, R.: Study on Sand Movement by Wind, *Report, Inst. Sci. Tech., Univ. Tokyo*, Vol. 5, No. 3/4, pp.95-112 , 1951 (in Japanese).
17. Nakagawa, H., Tsujimoto, T., Gotoh, H. and Watanabe, M.: Numerical simulation of bed-load layer: modeling of interaction among saltating particles, *Proc. Hydrol. Eng.*, JSCE, Vol. 37, pp. 605-610, 1993 (in Japanese).


## APPENDIX-NOTATION

*The following symbols are used in this paper:*

$A_2, A_3$ = two-and three-dimensional geometrical coefficients of particle, respectively;

$A_r$ = constant in logarithmic profile of the mean flow velocity;

$C_D, C_{D\infty}$ = drag coefficients;

$C_M$ = added mass coefficient;

$C_{1\varepsilon}, C_{2\varepsilon}$ = empirical constants in k-ε model (=1.44, 1.92);

$C_\mu$ = empirical constant in k-ε model (=0.09);

$D_w$ = damping factor for the modification of free surface of the flow (=0.8);

$d$ = diameter of particle;

$e, f$ = repulsive coefficients (=0.75);

$f_B$ = existing probability density of saltating particle;

$G$ = generation of turbulent energy;
$g$ = gravitational acceleration;
$H_s$ = average hight of saltation;
$h$ = water depth;
$k$, $k_p$ = turbulent energy and that at the lowest point of the grid, respectively;
$k_s$ = equivalent sand roughness;
$N_j$ = number of the saltating particles traversing $j$-th cell;
$P$ = pressure;
$q_B$ = sediment discharge;
$R_e$ = Reynolds number;
$R_j$ = coefficient of the change of particle's velocity due to interparticle collision;
$S_{PU}$, $S_{PV}$ = sink terms of the momentum equation for the interphase momentum transport;
$U$, $V$ = mean flow velocity in streamwise and upward vertical direction, respectively;
$U_m$ = balk mean velocity;
$U_p$ = mean velocity in the streamwise direction at the lowest grid point;
$u_p$, $v_p$ = velocity of the saltating particle in streamwise and upward vertical direction, respectively;
$u_{gin}$, $v_{gin}$ = velocity of the saltating particle just before a collision in streamwise and upward vertical direction, respectively;
$u_{gout}$, $v_{gout}$ = velocity of the saltating particle just after a collision in streamwise and upward vertical direction, respectively;
$u_*$ = dimensionless shear velocity;
$w_j$, $w_j^{cl}$ = coefficient for the distribution of sediment in $j$-th cell and that in clear water flow, respectively;
$x$, $y$ = coordinate in streamwise and upward vertical direction, respectively;
$y_p$ = height of the lowest grid point;
$\alpha$ = angle of hypothetical repulsing plane against the mean bed surface;
$\alpha_p$, $\beta_p$ = coefficients for the modification of interparticle collision;
$\Gamma$ = effective viscosity ;
$\Delta V_j$ = volume of $j$-th cell;
$\varepsilon$ ,$\varepsilon_p$ = energy dissipation and that at the lowest point of the grid, respectively;
$\theta$ = channel gradient;
$\kappa$ = Kármán constant;
$\nu$ = kinematic viscosity;
$\nu_t$ = kinematic eddy viscosity;
$\rho$ = mass density of fluid;
$\sigma$ = mass density of particle;
$\sigma_k$, $\sigma_\varepsilon$ = empirical constants of k-ε model (=1.0, 1.3); *and*
$\tau_*$ = dimensionless shear stress.

(Received April 20, 1994; revised December 2, 1994)